STUDY OF GAS FUEL LEAKAGE AND EXPLOSION IN THE ENGINE ROOM OF A SMALL LNG-FUELED SHIP

(DOI No: 10.3940/rina.ijme.2019.a3.541)

Q G Zheng and **W Q Wu,** Dalian Maritime University, China and **M Song,** Dalian Maritime University, MSA, Ministry of Transport, China

SUMMARY

The engine fuel piping in LNG-fuelled ships' engine room presents potential gas explosion risks due to possible gas fuel leakage and dispersion. A 3D CFD model with chemical reaction was described, validated and then used to simulate the possible gas dispersion and the consequent explosions in an engine room with regulations commanded ventilations. The results show that, with the given minor leaking of a fuel pipe, no more than 1kg of methane would accumulate in the engine room. The flammable gas clouds only exit in limited region and could lead to explosions with an overpressure about 12 mbar, presenting no injury risk to personnel. With the given major leaking, large region in the engine room would be filled with flammable gas cloud within tens of seconds. The gas cloud might lead to an explosion pressure of about 1 bar or higher, which might result in serious casualties in the engine room.

NOMENCLATURE

ρ	Density (kg m^{-3})
U	Velocity vector (m s^{-1})
S_ρ	Source term of mass (kg m^{-3} s^{-1})
y_m	Mass fraction of species
D_m	Diffusion coefficient of m
S_m	Source term for species m (kg m^{-3} s^{-1})
τ	Viscous stress tensor (N m^{-2})
S_U	Source term for momentum (N m^{-3})
C_p	Specific heat at a constant pressure (J kg^{-1} K^{-1})
T	Temperature (K)
p	Pressure (N m^{-2})
S_T	Source term for Temperature (N m^{-2} s^{-1})
μ	Effective viscosity (N m^{-2} s)
$\dot{\gamma}$	Rate of deformation tensor (s^{-1})
κ	Dilatational viscosity (N m^{-2} s)
δ	Unit tensor
q	Heat flux (J m^{-2} s^{-1})
k	Heat transfer coefficient (J m^{-2} K^{-1} s^{-1})
R	Gas constant of the mixture (J kg^{-1} K^{-1})
$\Re$	Universal gas constant (J mol^{-1} k^{-1})
M_m	Molecular weight of species m (kg kmol^{-1})
α	Mixture property such as C_p, μ, k,
α_m	Property of species m
S_k^v	Source term due to buoyancy and compressibility (J m^{-3} s^{-1})
μ_t	Turbulence viscosity (N m^{-2} s)
S_ε^v	Source term due to vegetation canopy (kg m^{-1} s^{-4})
v_i	stoichiometric coefficients for species i
R_{1i}	reactant i
R_{2i}	Product i
R_j	Reaction rate of reactant j (kg s^{-1})
M_i	Molecular weight of product i (kg kmol^{-1})
Q_{rj}	Heat of reaction j (J kg^{-1})
ω	Reaction rate (kg s^{-1})
S_L	Laminar burning velocity (m s^{-1})
I	Mean quench factor
Σ	Mean turbulent flamelet area (m^2)
g	Wave interval distribution depended front area (m^2)
σ_y	Flamelet orientation factor
L_y	Wrinkling degree of turbulent flame front
c	Overall progression variable
e	Expansion ratio
T_b	Temperatures of the burned gases (K)
T_u	Temperatures of unburned gases (K)
A_g	Grid flame surface area (m^{-2})
u_t	Turbulent burning velocity (m s^{-1})
r_0	Previous flame position form the centre of the ignition cell (m)
r	The new position after one time step later (m)

1. INTRODUCTION

Natural gas, with methane as the main composition, has been increasingly used as a clean fuel for ships propulsion since IGF code entered into force from 2017. Gas-fuelled ships may be of Gas safe machinery spaces or ESD (emergency shutdown) protected machinery spaces. In an ESD protected machinery space, a single failure might result in a gas release into the space. In a gas safe machinery space, failures more than a single might lead to a release of fuel gas into the machinery space (IMO, 2007). If a gas fuel leakage occurs in the engine room of an LNG powered ship, a gas explosion would occur with an ignition source. Sustained small leaks in low wind conditions may result very large clouds and lead to a severe explosion (Atkinson, et al, 2017). The accurate prediction of the overpressure value of the gas cloud explosion is of great significance for the assessment of the consequences of gas leakage accidents in the engine room of natural gas fuelled ships. The explosion consequences of flammable gas cloud are not only related to the gas cloud mass and concentration, but also closely related to the shape of the cloud, the distribution of built-in obstacles, the ignition position and other factors (Diakow, *et al*, 2018, Zhao, 1996, Moen, *et al*, 1980, Fa, *et al*, 2001 and Lin & Gui, 2002). As CFD (Computational Fluid Dynamics) based numerical simulation method can take into consideration various factors that have influence on gas cloud explosions with less cost and with no danger (Luo, *et al*, 2013 & Han, *et al*, 2016), numerical simulations of premixed methane-air cloud explosion in

medium and large scale vented spaces with different obstacle layouts were carried out in the paper. The CFD method and the CFD code of FLUIDYN were validated by the consistence between the simulation results and the experimental results. After that, the geometry model of a typical inland small LNG-fueled ship's engine room was established and explosions after the leakage of natural gas in this space were simulated. The study provides a numerical instrument to assess the risk of the natural gas fuelled ships' engine rooms.

2. CFD MODEL DESCRIPTIONS

2.1 CONSERVATION EQUATIONS

The process of gas combustion and explosion observes the conservation laws of mass, component, momentum and energy, respectively expressed as:

$$\frac{\partial \rho}{\partial t}+\nabla\cdot(\rho U)=S_{\rho} \tag{1}$$

$$\frac{\partial(\rho y_{\mathrm{m}})}{\partial t}+\nabla\cdot(\rho U y_{\mathrm{m}})=\nabla\cdot D_{\mathrm{m}}\nabla(y_{\mathrm{m}})+S_{\mathrm{m}} \tag{2}$$

$$\frac{\partial(\rho U)}{\partial t}+\nabla\cdot(\rho UU)=\nabla\cdot\tau-\nabla p+S_{\mathrm{u}} \tag{3}$$

$$\mathrm{C_p}\left[\frac{\partial(\rho T)}{\partial t}+\nabla\cdot(\rho UT)\right]=-\nabla\cdot q+\left[\frac{\partial p}{\partial \mathrm{t}}+U\cdot\nabla p\right]+\tau:\nabla U+S_{\mathrm{T}} \tag{4}$$

$$\tau=\mu\dot{\gamma}-\left(\tfrac{2}{3}\mu-\kappa\right)(\nabla\cdot U)\delta \tag{5}$$

$$q=-k\nabla T \tag{6}$$

2.2 THERMODYNAMIC MODEL

Ideal gas law is used for the thermodynamic model of mixture of gases. The gas law and the calculation of the mixture parameters are as follows:

$$p=\rho RT \tag{7}$$

$$R=\Re\sum_{\mathrm{m}}\frac{y_{\mathrm{m}}}{M_{\mathrm{m}}} \tag{8}$$

$$\alpha=\sum_{\mathrm{m}}\alpha_{\mathrm{m}}y_{\mathrm{m}} \tag{9}$$

2.3 TURBULENCE MODEL

In combustion simulation, the following k-ε turbulence model is used to simulate the turbulence flow:

$$\frac{\partial(\rho k)}{\partial t}+\nabla\cdot(\rho Uk)=\nabla\cdot\left(\mu+\frac{\mu_{\mathrm{t}}}{\sigma_{\mathrm{k}}}\right)\nabla k+P_{\mathrm{k}}+P_{\mathrm{b}}-\rho\varepsilon-\tfrac{2}{3}\rho k\nabla\cdot U+S_{\mathrm{k}}^{\mathrm{v}} \tag{10}$$

$$\frac{\partial(\rho\varepsilon)}{\partial t}+\nabla\cdot(\rho U\varepsilon)=\nabla\cdot\left(\mu+\frac{\mu_{\mathrm{t}}}{\sigma_{\varepsilon}}\right)\nabla\varepsilon+\frac{\varepsilon}{k}\left[\mathrm{C_{\varepsilon 1}}(P_k+P_b)-\mathrm{C_{\varepsilon 2}}\rho\varepsilon\right]-$$

$$\left(\tfrac{2}{3}\mathrm{C_{\varepsilon 1}}-\mathrm{C_{\varepsilon 3}}\right)\rho\varepsilon\nabla\cdot U+S_{\varepsilon}^{\mathrm{v}} \tag{11}$$

2.4 CHEMICAL REACTION MODEL

2.4 (a) Chemical Reaction Equations

Chemical reaction of the methane is described as (12), Reactant source term and temperature source term are expressed as (13) and (14).

$$\sum_{i=1}^{i=j}\nu_{1i}R_{1i}\longleftrightarrow\sum_{i=1}^{i=k}\nu_{2i}R_{2i} \tag{12}$$

$$S_i=\sum_j R_j\left(\nu_{2i}-\nu_{1i}\right)M_i \tag{13}$$

$$S_T=\frac{1}{\mathrm{C_p}}\sum_{\mathrm{j}}Q_{\mathrm{rj}}R_{\mathrm{j}} \tag{14}$$

2.4 (b) Reaction Rate

Introduce the SIF (**Simple Interface Flame**) flame model (Arntzen, 1998) to the BML (Bray-Moss-Libby) combustion model (Bailly, Champion & Garreton, 1997), and regard the combustion as two parts of flame combustion and turbulent motion, then the reaction rate ω is expressed as:

$$\omega=\rho_{\mathrm{k}}S_{\mathrm{L}}I\Sigma \tag{15}$$

$$\Sigma=\frac{g}{\sigma_y L_y}(1+\tau)\frac{c(1-c)}{(1+ec)^2} \tag{16}$$

$$e=\frac{T_{\mathrm{b}}}{T_{\mathrm{u}}}-1 \tag{17}$$

An algebraic relation is used for mean flamelet area based up on flamelet fast chemistry assumptions, assuming the characteristic life time of a strained packet of fresh reactants is proportional to the turbulence characteristic time scale. Define the normalized stretch rate Γ_{k} (Bradley, Gaskell & Gu, 1994) and normalized density $\bar{\rho}$ as follows:

$$\overline{\rho}=\frac{\rho_{\mathrm{R}}}{1+ec} \tag{18}$$

$$\Gamma_{\mathrm{k}}=\frac{S_{\mathrm{L}}I/L_y}{\varepsilon/k} \tag{19}$$

Take g/L_{y} as an empirical coefficient $\mathrm{C_1}$, replace ε/k with $A_{\mathrm{g}}u_{\mathrm{t}}$, then the reaction rate ω is rewritten as:

$$\omega=\mathrm{C_1}\overline{\rho}\Gamma_{\mathrm{k}}A_{\mathrm{g}}u_{\mathrm{t}}(1+e)\frac{c(1-c)}{(1+ec)} \tag{20}$$

2.4 (c) Ignition Rate

In the ignition cells, the laminar flame speed is assumed, as can be handled even in very coarse mesh ignition cells. The initial flame radius is zero and final radius is limited

to the particular cell size. The reaction rate in the ignition cell is calculated as follows:

$$\omega = \frac{\frac{4}{3}\pi\left(r^3 - r_0^3\right)}{Vdt} \tag{21}$$

$$r = r_0 + S_L dt \tag{22}$$

3. CFD MODEL VALIDATIONS

Considering the strengthening effect of obstacles in the gas cloud on flame propagation (Ciccarelli, Johansen & Parravani, 2010), the following two sets of explosion experiments of premixed methane gas cloud with built-in complex obstacles were simulated, the flame propagation and overpressure values were compared.

3.1 VALIDATION IN MEDIUM SCALE SPACE

3.1 (a) Simulation Description

The premixed methane-air cloud in a container with obstacles is established as the numerical simulation physical model. The dimension inside the containers is of a rectangular cross section of 150 mm×150 mm with a height of 500 mm. The lower end is closed, the upper end is open, and three obstacles of 150 mm×75 mm×10 mm are distributed inside as shown. In order to prevent the gas cloud from escaping to the outside, the open end is sealed with a plastic membrane. The ignition point and the pressure monitoring point are located near the lower end surface (Wen, Yu & Liu, 2013).

The computational domain is divided into structured meshes. The mesh size inside the congested space is all of 5mm, but of 3mm beside the obstacles. The open outer space adopts a coarser mesh (with a factor of 1.03).

To verify the computed results with the experimental results, the parameters in the numerical simulation are set the same as the experimental parameters. The gas cloud is set to 9.5% by volume concentration of methane, the initial temperature is set to 300K, and the initial velocity is set to a small initial velocity close to static (0.001 m/s). As the reaction time is short (less than 50 ms), the surface of the container and of the obstacles is treated as the adiabatic wall. The plastic membrane is set as a conditional boundary depending to surface overpressure. The boundary of the outer calculation domain is set as pressure static, where it's treated as zero pressure gradients when the calculated inside pressure is higher than the boundary pressure, and is treated as static pressure boundary (pressure inlet) when the calculated inside pressure is lower than the setting.

Configuration 1 was simulated with 3 different time steps (0.05ms, 0.02ms, and 0.01ms), by CFD software Fluidyn, which incorporated the above described models. The maximum overpressures simulated with time step of 0.05 ms is 15% lower than that with 0.01ms, while the result with 0.02ms is 4% lower than that with 0.01ms. In order to save the calculation cost, other simulations were carried out with a time step of 0.02ms.

3.1 (b) Results Contrast to Experiments

As Figure 1 shows, the flame propagation from simulated results (lower part) is highly consistent with that from experiments (upper part) (Wen, Yu & Liu, 2013).

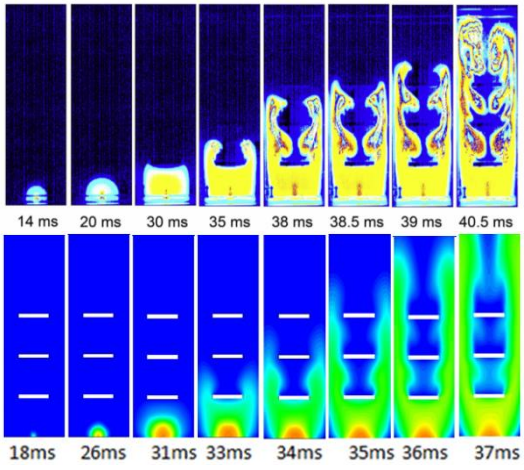

Configuration 1

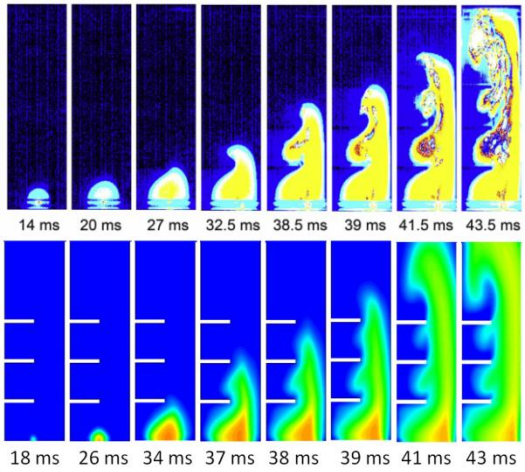

Configuration 2

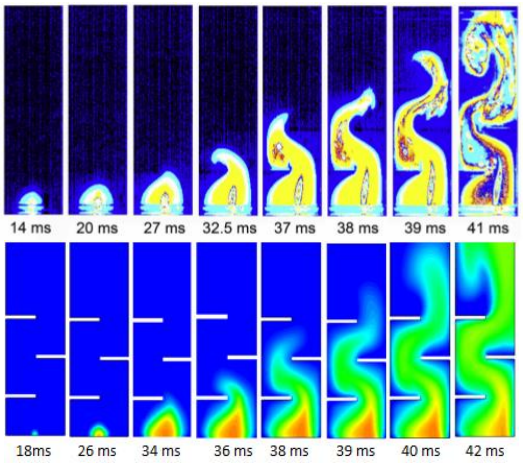

Configuration 3

Figure 1: Comparison of the flame propagation

Figure 2 illustrates the pressure-time curves from the experimental results and the numerical calculation for three different obstacle arrangements. P_v is the pressure of the monitoring point just before the membrane broken.

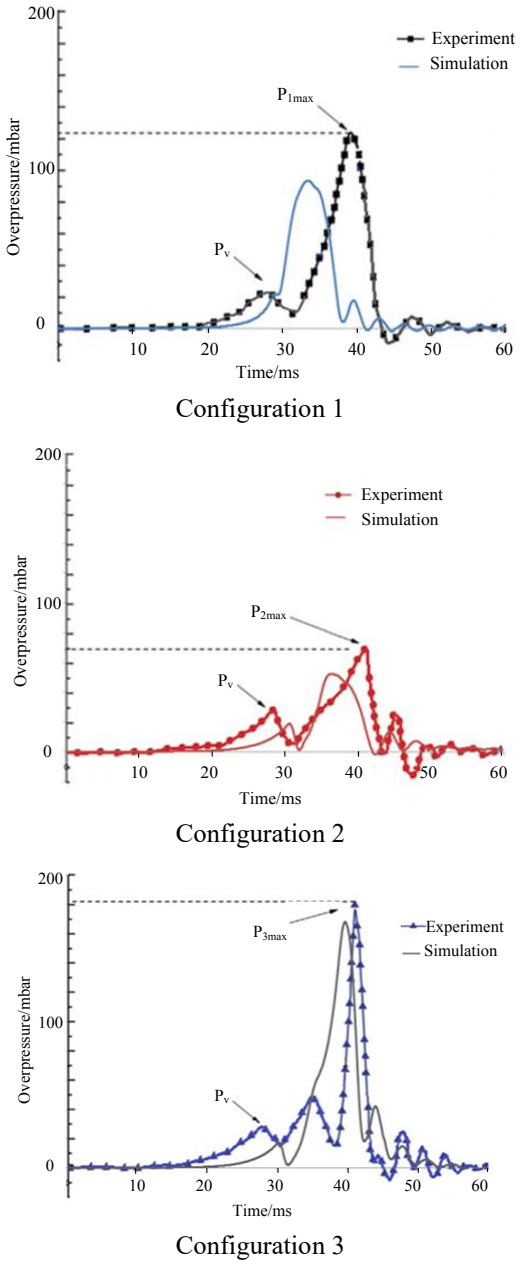

Figure 2: Comparison of numerical and experimental results

By comparing the three sets of data in the medium scale, it can be found that the numerical results change with the obstacle arrangement at a same trend as the experimental results do. When the three obstacles are staggered on two sides, the maximum overpressure value reaches the highest value of 168 mbar. The main reasons include perturbation to the flame and the increased flow resistance caused by the staggered obstacles. When the three obstacles are on the same side, the maximum overpressure is only 52 mbar. The reason is that the explosion pressure initiated from the ignition position is released through the side without obstacles and the methane between the obstacles burns after the maximum explosion pressure and does not contribute to the maximum overpressure. When all three obstacles are in the middle position, the maximum overpressure is 93 mbar.

3.2 VALIDATION OF LARGE SCALE

3.2 (a) Simulation Description

Considering the actual size and pressure relief conditions of the small ship's machinery space, the experiments carried out by G. Tomlin et al, (2015), were selected as the large-scale validation experiments to simulate. The space dimension is 9.0m×4.5m×4.5m, the area ratio of the pressure relief is 1, 2, 4, and 9 respectively. The built-in obstacles are horizontally placed cylinders with a diameter of 0.18m. In configuration (a), 12 pieces of obstacles make an area blockage rate of 12% and a volume blockage of 0.75%. In configuration (b), 20 pieces of obstacles make an area blockage of 20% and a volume blockage of 1.26%.

Configuration (a) is meshed to 91496 unstructured elements. Configuration (b) is meshed with 104264 unstructured elements. The distance between the nodes on edge is 0.1m; the meshes outside the constrained space are a little bigger.

To verify the time step is suitable, the configuration (b) was simulated with three different time steps of 1ms, 0.5ms and 0.2ms, with relief area ratio being set to 4. The maximum overpressures calculated with time step of 1 ms is about 3% lower than that with 0.2ms, the result with 0.5ms is about 1% lower than that with 0.2ms. In order to save the calculation cost, other simulations were carried out with the time step of 1ms.

3.2 (b) Results Contrast to Experiments

The numerical results as well as the experimental results show that, the smaller pressure relieving area results in the higher maximum overpressure with the same obstacle configuration, and the higher blockage rate results in the higher maximum overpressure with the same pressure relieving area. The contrast of overpressure-time profiles is as shown in Figure 3. The maximum pressure occurrence time in the numerical simulation is slightly earlier than the experimental result, and this deviation is consistent with the deviation in the medium scale experiments validations.

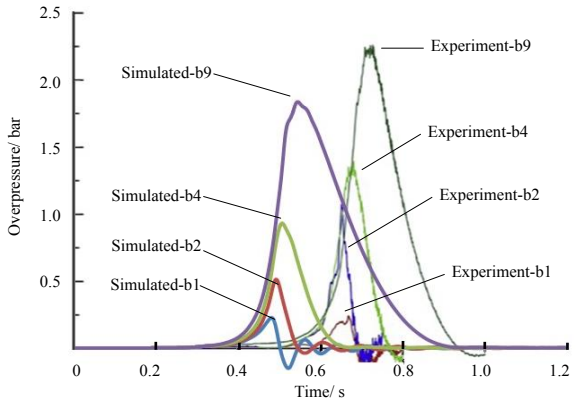

Figure 3: Comparison of overpressure-time profile for configuration (b)

3.3 VALIDATION ANALYSIS

Table 1 shows the maximum overpressure comparisons between experiments and numerical simulations. The numerical results are generally slightly lower than the experimental results. The overpressure ratio of simulations to experiments is steadily distributed in the range of 0.47-0.95, while the major is in the interval of 0.7-0.95. The reason for the deviation lies in that, the initial/boundary condition setting might be different from the actual situation, and the standard k-ε turbulence model has insufficient calculation of the flow around the cylinder and perhaps does not fully reflect the flame propagation enhancement by the cylindrical obstacles.

According to the deviation in validations, it can be considered that the maximum overpressure value in the simulation results may be relatively a little lower, and the maximum overpressure occurrence time may be a little earlier, compared to the actual time.

Table 1: The comparison of maximum overpressure

Cases	Experimental	Simulated	Ratio
Configuration 1	124	93	0.75
Configuration 2	69	52	0.75
Configuration 3	183	168	0.92
Configuration a1	157	123	0.78
Configuration a2	677	408	0.60
Configuration a4	1058	777	0.67
Configuration a9	1598	1523	0.73
Configuration b1	246	226	0.95
Configuration b2	1079	512	0.47
Configuration b4	1397	933	0.67
Configuration b9	2134	1839	0.86
average			0.765

4. GAS EXPLOSIONS IN ENGINE ROOM

4.1 DESCRIPTION OF GEOMETRY AND MESH

The engine room of typical inland small-sized LNG power ship is the space where the leakage, dispersion and explosion supposed to happen. As shown in Figure 4, the dimension is 11.8m×8.4m×3.5m., with internal layouts mainly including medium-speed propulsion diesel engines, power generation diesel engines, air compressors, air bottles and other equipment (Wen, Yu & Liu, 2013). The space is meshed with 149,020 unstructured elements, with node distance of 0.2m to 0.25m on ship structure and node distance of 0.1m on the equipment surfaces.

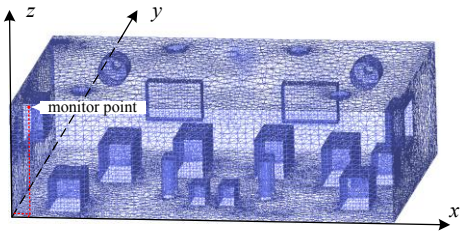

Figure 4: Meshing of the engine room

4.2 SCENARIOS AND SETTINGS

4.2 (a) Quasi-steady Ventilation Field

According to IGF code, the engine room should be draught vented of 30 air changes per hour and a quasi-steady field is achieved after 10 minutes of ventilation. So the air outlet is set to flow outlet boundary condition of 2.778m^3/s, and the air inlet is set to pressure static boundary. Taking into consideration the impact of the air consumption of the diesel engines on the velocity field, the engine suction is set as flow outlet of 0.85m^3/s, ignoring the impact of other air consumption. The surfaces are set to isothermal wall at temperature of 330K or 308K respectively, according to its normal temperature under working condition.

4.2 (b) Leakage and Dispersion

The above quasi-steady field is used as the initial conditions, and methane is used instead of natural gas in the leakage simulation. According to the fuel supply piping arrangement in the engine room, three points L1(0.1,1.2,2.2), L2(0.1,7.5,3.0) and L3(5.7,8.4,3.0) are selected as the different leaking positions. Considering the possible different damage degree of the gas supply pipes, the leaking flow rate is set to 0.008267 kg/s and 0.13228 kg/s respectively standing for minor sealing failures and major ruptures (Wen, Yu & Liu, 2013).

4.2 (c) Gas Cloud Explosions

Results of gas leakage and dispersion were set as the initial conditions for explosion simulations and an ignition point was set in the flammable concentration area, the boundary conditions kept unchanged. The explosions were simulated with different leaking duration. The durations of small leaks are decided by simulation results in the following *section 4.3*, the durations of big flow rate of leaks are decided by taking reference to literature (Li, Zhou & Konovessis, 2016) and the assumption of a possible quick shutdown of the leakage.

4.3 RESULTS AND DISCUSSION

4.3 (a) Slow Leakage

The leakage monitoring system might not reliably detect the small leakage (Li, Zhou & Konovessis, 2016), so the leaks were simulated until the gas accumulation amount nearly no longer increasing (ventilation discharging about 99% of the leakage and the accumulation increasing less than 0.0001kg/s). Thus the accumulated methane amount is 0.354kg, 0.703kg, and 0.848kg, respectively for 280s, 380s, and 470s of leakage from L1, L2, and L3. The concentration distribution is as shown in Figure 5.

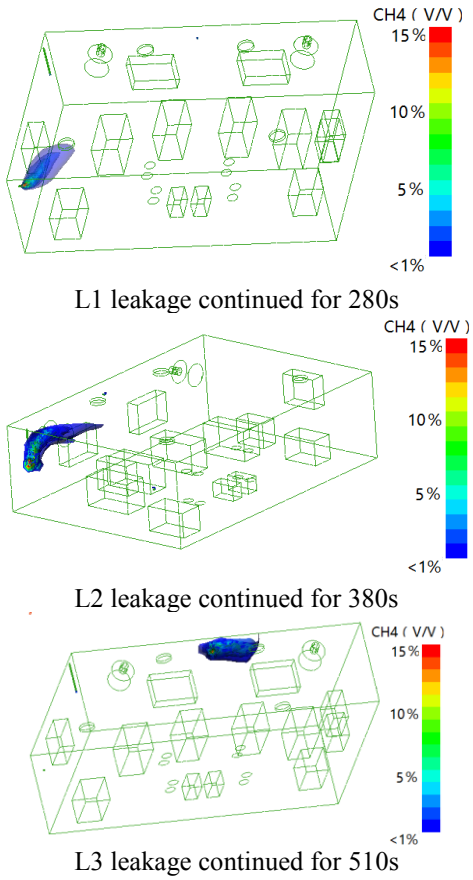

Figure 5: Methane concentration distribution after small leakage

Because of the comparatively small venting area to the space volume, the pressures of multiple points monitored in the explosion simulations show nearly no difference to each other except a certain time difference. Figure 6 shows the overpressure-time profile for the monitoring point at (0.5, 0.5, 3.3). The maximum explosion overpressures of the gas clouds leaking from L1, L2, and L3 are 11.4 mbar, 5.5 mbar and 8.7 mbar respectively. Though a larger amount of accumulated methane in the engine room from L2 and L3 leakage, the gas cloud did not produce a higher explosion pressure than that formed by the L1 leakage. Reasons accounting for this might be: the gas clouds leaking from L2 and L3 distributed over a larger space range and the amount of gas in the optimal concentration range is small; the larger deviation from the optimal concentration, the slower the reaction is in the reaction speed model (see equation 20). In the presence of a pressure relieving port, part of the methane reaction does not contribute to the maximum overpressure.

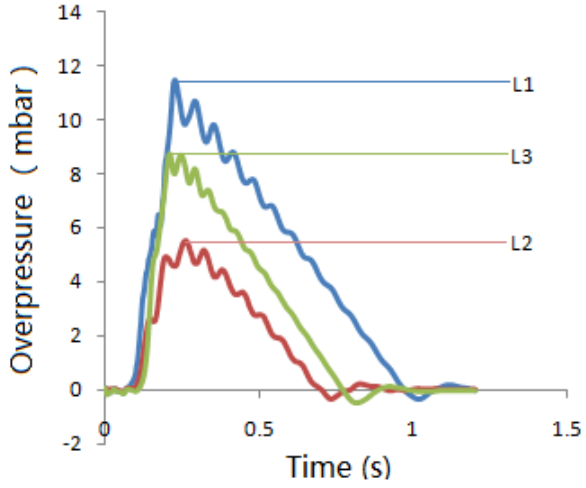

Figure 6: Overpressure-time profile for the explosion of continuous small leakage

4.3 (b) Big Flow Rate Leakage

30s of big leakage from L1, L2 and L3 respectively resulted in a methane accumulation of 3.03kg, 3.46kg and 3.31kg in the engine room, which accounting for 76%, 87% and 83% of the total leakage. 60s of big leakage from L1, L2 and L3 respectively resulted in a methane accumulation of 5.20kg, 6.24kg and 5.74kg, the accumulation ratios being 65%, 79% and 72% respectively. This indicates that the ventilation of 30 changes per hour, as required by IGF code, is not effective in preventing the gas accumulation from a big leakage. Within tens of seconds, a big leakage could result in a large space in the engine room filled with flammable cloud. Figure 7 shows the concentration isosurfaces for 60s big leakage.

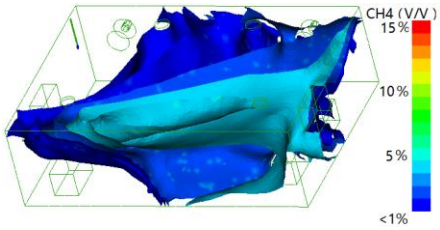

For L1 leakage

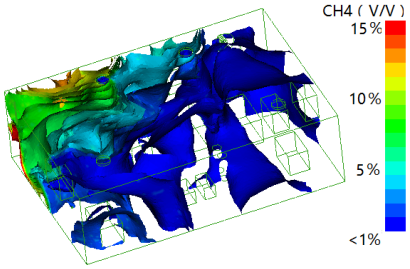

For L2 leakage

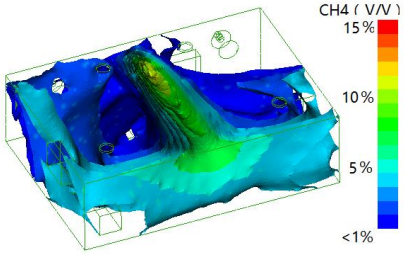

For L3 leakage

Figure 7: Methane concentration distribution for 60s big leakage

The maximum overpressures of 30s big leaks explosions are respectively 0.85 bar, 0.99 bar and 0.91 bar, at 0.22s, 0.21s and 0.20s respectively. For explosion of 60s big leakage, the overpressure reached a maximum value of 1.68 bar, 2.08 bar and 1.79 bar at about 0.2s, which would result in personnel death in engine room (Richmond, Yelverton & Fletcher, 1986). The overpressure-time profile is as shown in Figure 8. Considering the discrepancy in validation in *Section 3*, the actual pressure might be slightly higher than the above calculated results, and the maximum overpressure time is slightly later than 0.2s.

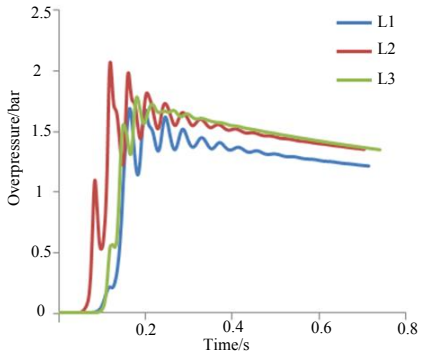

Figure 8: Overpressure-time profiles for 60s leakage explosion

Figure 9 shows the amount of methane accumulation and its corresponding explosion overpressure. By fitting the data, it can be seen that in this amount range of methane, the maximum overpressure value is in highly linear relationship with the accumulated methane mass. The reasons lie in: 1) the accumulated methane is about 20% of the total amount at equivalent concentration of the whole engine room space (23.5 kg), i.e., the flammable cloud is at rich oxygen condition and the accumulated methane could be completely oxidized; 2) the explosions take place in the same space with the same obstacle distribution, the similar velocity field, and the similar concentration distribution, which means the similar reaction speed distribution.

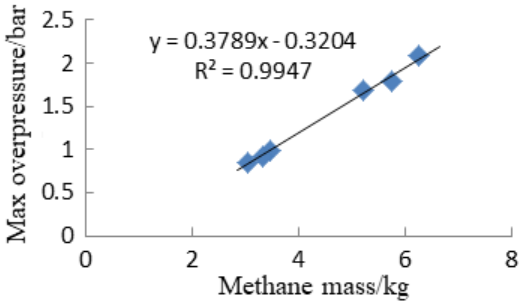

Figure 9: The accumulated methane and corresponding overpressure

5. CONCLUSIONS

The simulated results are in good agreement with that from the experiments, showing that CFD code with BML combustion and SIF flame model can give creditable simulation which may reflect the influence of the obstacle layout and the pressure relieving area to the flame propagation and to the overpressure of methane explosions in congested spaces.

The simulations of the leakage in the engine room show that under ventilation conditions required by the IGF Code: a) small rate leakages lead to little accumulation and presents no danger even the explosions take place; b) big rate leakages could result in large flammable gas cloud formed in the engine room within tens of seconds, and the explosion of the gas cloud resulted from 60s' leakage might produce a overpressure over 1 bar, which is fatal for persons in engine room.

In conditions with same ventilations and obstacles, the cloud explosion overpressure is highly proportional to the mass of the fuel gas.

6. ACKNOWLEDGEMENTS

Experimental results used for contrast in Figure 1 and Figure 2 are cited from Wen, Yu & Liu, 2013, and those used in Figure 3 are cited from Tomlin, *et al*, 2015.

7. REFERENCES

1. IMO. *IGF Code*, 2017
2. ATKINSON, G., COWPE, E., HALLIDAY, J., PAINTER, D. (2017) *A review of very large vapour cloud explosions: Cloud formation and explosion severity*. Journal of Loss Prevention in the Process Industries, 2017, 48:367-375.
3. DIAKOW, P.A., THOMAS, J.K., VIVANCO, E. (2018) *Comparison of large-scale vented deflagration tests to CFD simulations for partially congested enclosures.* Journal of Loss Prevention in the Process Industries, 2018, 56:147 -154.
4. ZHAO, HY. (1996) *Explosion principle of gas and dust*. Beijing Institute of Technology Press, Beijing. 9787810450799
5. MOEN, I.O., DONATO, M. KNYSTAUTAS, R. LEE, J.H. (1980) *Flame acceleration due to turbulence produced by obstacles*. Combustion and Flame, 1980, 39:21-32.
6. FAN, WJ., SUN, WC., WU, CK. (2001) *A Study on Flame Propagation in a Gas-Explosion Ash Remover*. Journal of Combustion Science and Technology, 2001, 7(4): 217-220.
7. LIN, BQ. and GUI, XH. (2002) *Numerical Simulation Research on Flame Transmission in Gas Explosion*. Journal of China University of Mining & Technology, 2002, 31(1):6-9.
8. LUO, ZM., ZHANG, Q., WANG, H., CHENG, FM. (2013) *Numerical simulation of gas explosion in confined space with FLACS*, JOURNAL OF CHINA COAL SOCIETY, 2013, 8: 1381-1387.
9. HAN L., LIU, XP., MA, JJ., GUO, KH. (2016) *Study on consequence of LNG leakage in semi-confined space based on CFD*, Journal of Safety Science and Technology, 2016, 06:110-115.
10. ARNTZEN, B.J. (1998) *Modelling of Turbulent and combustion for simulation of gas explosions in complex geometries*. The Norwegian University of Science and Technology, 1998.
11. BAILLY, P., CHAMPION, M., GARRETON, D. (1997), *Counter-gradient diffusion in a confined turbulent premixed flame*, Phys, Fluids, 1997, 9(3):766-775.
12. BRADLEY, D. GASKELL, P.H., GU, X.J. (1994) *Application of a Reynolds Stress, Stretched Flamelet, Mathematical Model to Computations of Turbulent Burning*. Combustion and Flame 1994, 96: 221-248.
13. CICCARELLI, G., JOHANSEN, C.T., PARRAVANI, M. (2010) *The role of shock flame interactions on flame acceleration in an obstacle laden channel.* Combustion and Flame, 2010, 157: 2125-2136.
14. WEN, XP., YU, MG., LIU, ZC. (2013) *Effects of cross-wise obstacle position on methane-air deflagration characteristics*. Journal of Loss Prevention in the Process Industries, 2013, 26:1335-1340.
15. TOMLIN, G., JOHNSON, D.M., CRONIN, P., PHYLAKTOU, H.N., ANDREWS, G.E. *The effect of vent size and congestion in large-scale vented natural gas/air explosions*. Journal of Loss Prevention in the Process Industries, 2015, 35:169-181.
16. LI, XJ., ZHOU, RP., KONOVESSIS, D. (2016). *CFD analysis of natural gas dispersion in engine room space based on multi-factor coupling*. Ocean Engineering, 2016, 111:524-532
17. RICHMOND, D.R., YELVERTON, J.T., FLETCHER, E.R. (1986) *New air blast criteria for man*. DOD Explosives Safety Seminar 22ed, 1986.